Characterisation of deuterium distributions in corroded zirconium alloys using high-resolution SIMS imaging

Junliang Liu[1], Kexue Li[1,2,*], James Sayers[1], Thomas Aarholt[1,3], Guanze He[1], Helen Hulme[2,4], Alistair Garner[2], Michael Preuss[2], Heidi Nordin[5], Jonna M. Partezana[6], Magnus Limbäck[6], Sergio Lozano-Perez[1], Susan Ortner[7], Chris R.M. Grovenor[1]

[1]Department of Materials, University of Oxford, Parks Road, OX1 3PH, Oxford, UK.

[2]Department of Materials, University of Manchester, Oxford Road, Manchester, M13 9PL, UK.

[3]Department of Physics, University of Oslo, Oslo 0316, Norway.

[4]Jacobs, Walton House, Birchwood, WA3 6GA, UK.

[5]Canadian Nuclear Laboratories, Chalk River, ON K0J 1J0, Canada.

[6]Westinghouse Electric Sweden AB, SE-721 63 Västerås, Sweden.

[7]National Nuclear Laboratory, Culham Science Centre, Abingdon, Oxon, OX14 3DB, UK.

[*]Corresponding author: E-mail address: kexue.li@manchester.ac.uk (Kexue Li)

Table S1. Water chemistry of in-flux and out-of-flux corrosion tests of CNL Zr-2.5Nb alloys.

Parameters	Required values
Dissolved D_2	5-7 Nml/kg D_2O
Dissolved O_2	< 5 ppb
Li^+ concentration	0.9-1.3 ppm
$pH_{20°C}$	10.6-10.8
Cl^- concentration	<0.1 mg/kg D_2O
Suspended solids	<0.1 mg/kg D_2O
Conductivity	5-15 mS/cm

Table S2. NanoSIMS analysis in each alloy and the tuning parameters.

Sample ID	File Name	Raster size (µm)	Pixels	Planes	depth (µm)	Dwell time (µs/pixel)	Primary beam (pA)	Masses
Cs$^+$ primary ion beam, Zircaloy-4								
Z4-1	201610_3	5×5	256×256	200	1.8	5000	-	^{2}D$^-$, ^{18}O$^-$
Z4-1	201610_4	5×5	256×256	250	1.8	5000	-	^{2}D$^-$, ^{18}O$^-$
Z4-1	201610_5	5×5	256×256	250	1.8	5000	-	^{2}D$^-$, ^{18}O$^-$
Z4-1	201705_11	10×10	512×512	3100	1.9	300	-	^{2}D$^-$, ^{18}O$^-$
Z4-1	201705_12	10×10	512×512	785	0.6	300	-	^{2}D$^-$, ^{18}O$^-$
Z4-1	201706_1	10×10	512×512	2755	1.9	1200	-	^{52}Cr^{16}O$^-$, ^{56}Fe^{16}O$^-$, ^{58}Ni^{16}O$^-$
Z4-2	201703_1	10×10	512×512	2560	2.2	300	2.1	^{2}D$^-$, ^{16}O$^-$
Z4-2	201610_16	5×5	256×256	500	2.2	2000	-	^{2}D$^-$, ^{18}O$^-$
Z4-2	201610_17	5×5	256×256	500	2.2	2000	-	^{2}D$^-$, ^{18}O$^-$
Z4-2	201610_18	5×5	256×256	500	2.2	2000	-	^{2}D$^-$, ^{18}O$^-$
Z4-2	201802_9	10×10	256×256	2000	~1	500	3.6	^{1}H$^-$, ^{2}D$^-$
Z4-2	201802_10-12*	10×10	256×256	160	~0.02	1000	1.5	^{52}Cr^{16}O$^-$, ^{56}Fe^{16}O$^-$, ^{58}Ni^{16}O$^-$, ^{120}Sn$^-$
Z4-2	201802_13	10×10	256×256	225	~0.12	500	3.6	^{1}H$^-$, ^{2}D$^-$
Z4-pH-1	201610_1	5×5	256×256	250	1.47	5000	-	^{2}D$^-$, ^{18}O$^-$
Z4-pH-1	201610_2@1	5×5	256×256	250	1.47	5000	-	^{2}D$^-$, ^{18}O$^-$
Z4-pH-1	201610_2@2	5×5	256×256	250	1.47	5000	-	^{2}D$^-$, ^{18}O$^-$
Z4-pH-2	201609_16	5×5	256×256	400	2.93	5000	-	^{2}D$^-$, ^{18}O$^-$
Z4-pH-2	201609_19	5×5	256×256	400	2.93	5000	-	^{2}D$^-$, ^{18}O$^-$
Z4-pH-2	201609_20	5×5	256×256	400	2.93	5000	-	^{2}D$^-$, ^{18}O$^-$
Cs$^+$ primary ion beam, Zr-1Nb								
1Nb-1	201611_29@1_1	5×5	256×256	600	2.4	2000	-	^{2}D$^-$, ^{18}O$^-$
1Nb-1	201611_29@1_2	5×5	256×256	600	2.4	2000	-	^{2}D$^-$, ^{18}O$^-$
1Nb-1	201611_29@1_3	5×5	256×256	600	2.4	2000	-	^{2}D$^-$, ^{18}O$^-$
Cs$^+$ primary ion beam, Zr-2.5Nb								
2.5Nb-1	201804_30@1_1	5×5	256×256	1000	1.9	1000	-	^{2}D$^-$, ^{18}O$^-$
2.5Nb-1	201804_30@1_2	5×5	256×256	1000	1.9	1000	-	^{1}H$^-$, ^{2}D$^-$
2.5Nb-1	201804_30@1_3	5×5	256×256	1000	1.9	1000	-	^{1}H$^-$, ^{2}D$^-$
2.5Nb-1	201804_30@1_4	5×5	256×256	1000	1.9	1000	-	^{1}H$^-$, ^{2}D$^-$
2.5Nb-1	201802_8	10×10	256×256	4025	1.9	300	2.5	^{1}H$^-$, ^{2}D$^-$
2.5Nb-2	201805_1@1_1	5×5	256×256	1000	3.08	2000	1.85	^{1}H$^-$, ^{2}D$^-$
2.5Nb-2	201810_21	10×10	256×256	4300	<3.1	1000	1.6	^{16}O$_2^-$, ^{56}Fe^{16}O$^-$, ^{93}Nb^{16}O$^-$
2.5Nb-2	201810_22	5×5	256×256	2500	<3.1	1000	1.6	^{16}O$_2^-$, ^{56}Fe^{16}O$^-$, ^{93}Nb^{16}O$^-$
2.5Nb-3	201808_19	8×8	256×256	3700	2	1000	2	^{2}D$^-$, ^{18}O$^-$
2.5Nb-3	201811_23	8×8	256×256	4000		1000	1.9	^{1}H$^-$, ^{2}D$^-$
2.5Nb-4	201811_5	8×8	256×256	5000		1000	1.9	^{1}H$^-$, ^{2}D$^-$

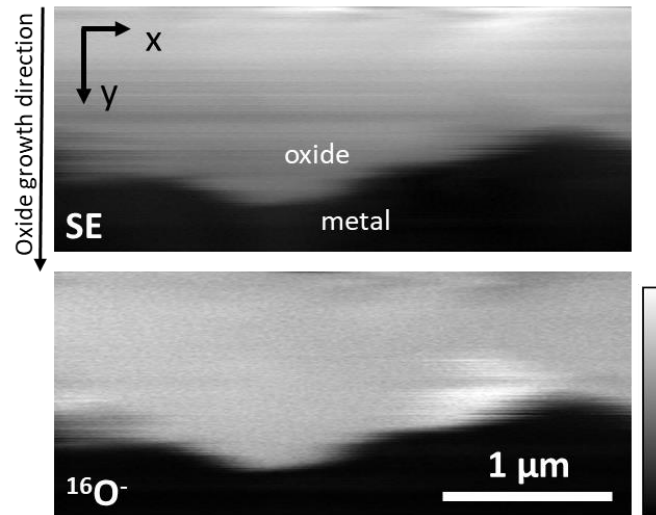*** D1 aperture is set to 3 (150 µm in diameter) and other measurements are set to D1-2 (300 µm in diameter).**

Figure S1. NanoSIMS SE and $^{16}O^-$ maps from a Zircaloy-4 sample showing the metal/oxide interface
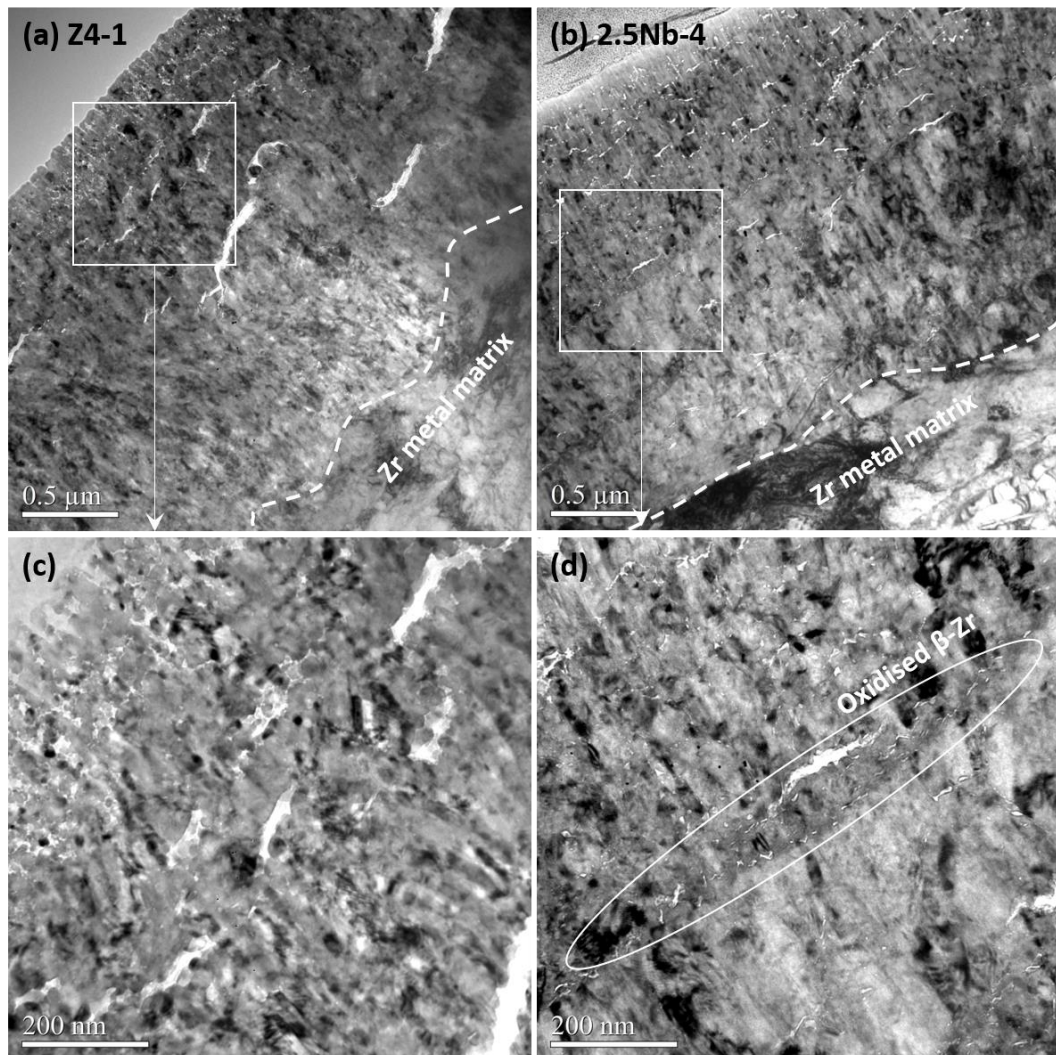

Figure S2. TEM Fresnel contrast images from (a and c) Z4-1 and (b and d) 2.5Nb-4 showing the distribution of nano-porosity as a function of depth through the oxide. The oxide/metal interface in (a and b) is marked by white dashed lines. Δf = -2000 nm in (c and d) so the porosity shows as white contrast. The region of an oxidised β-Zr plate is marked in (d).
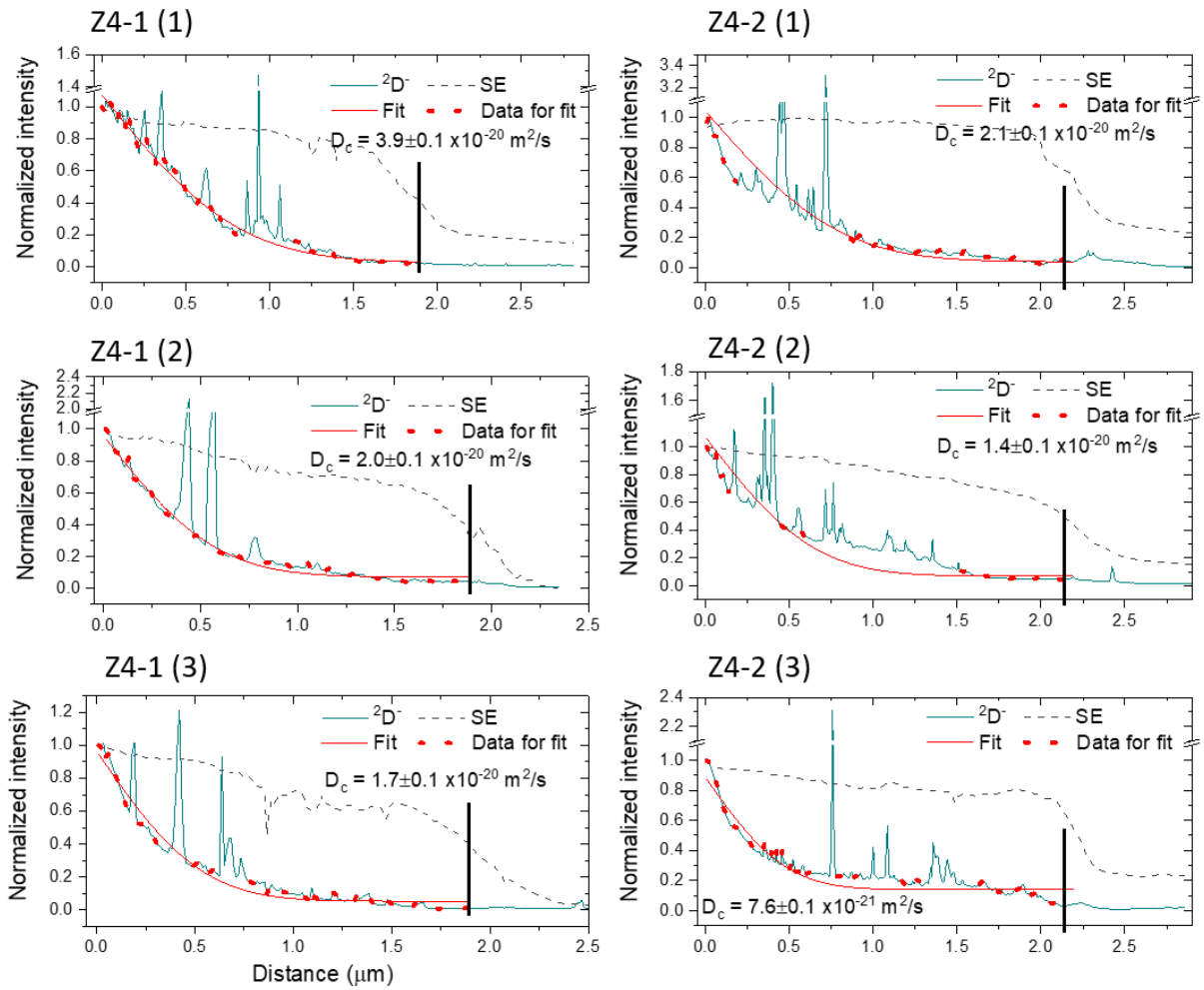
Figure S3. NanoSIMS Depth profile data in samples Z4-1 (left column, 61-days autoclave-corroded Zircaloy-4) and Z4-2 (right column, 106-days autoclave-corroded Zircaloy-4).

Figure S4. NanoSIMS Depth profile data in samples Z4-pH-1 (left column, 61-days high-pH autoclave-corroded Zircaloy-4) and Z4-pH-2 (right column, 147-days high-pH autoclave-corroded Zircaloy-4).
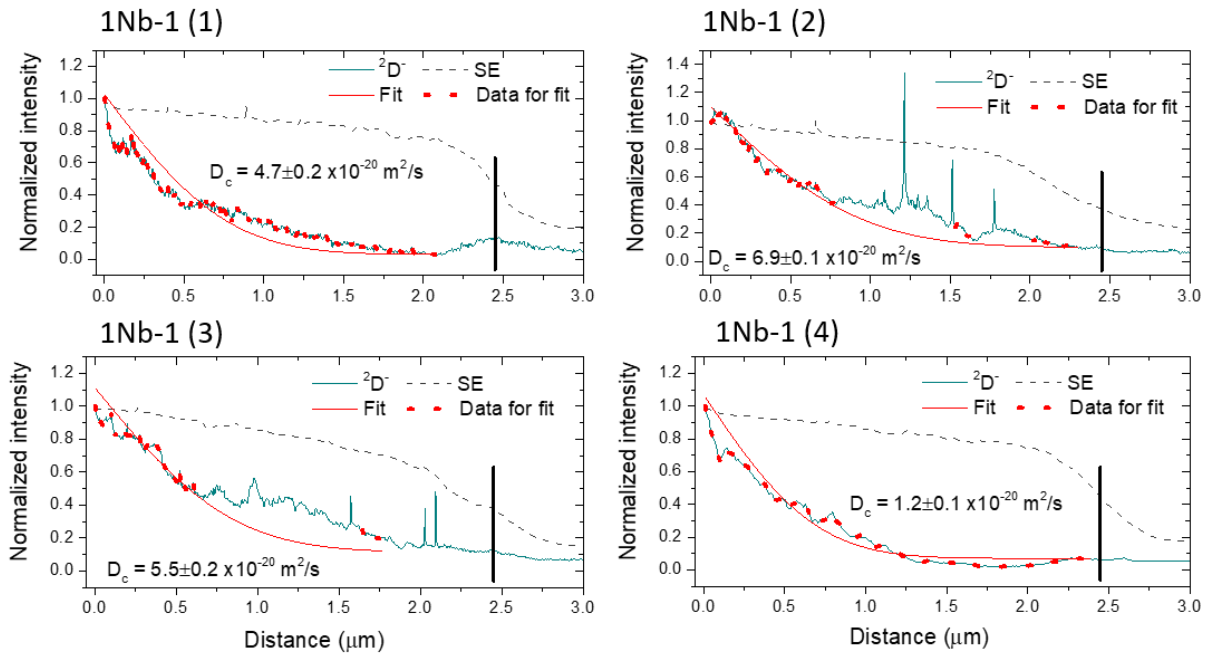

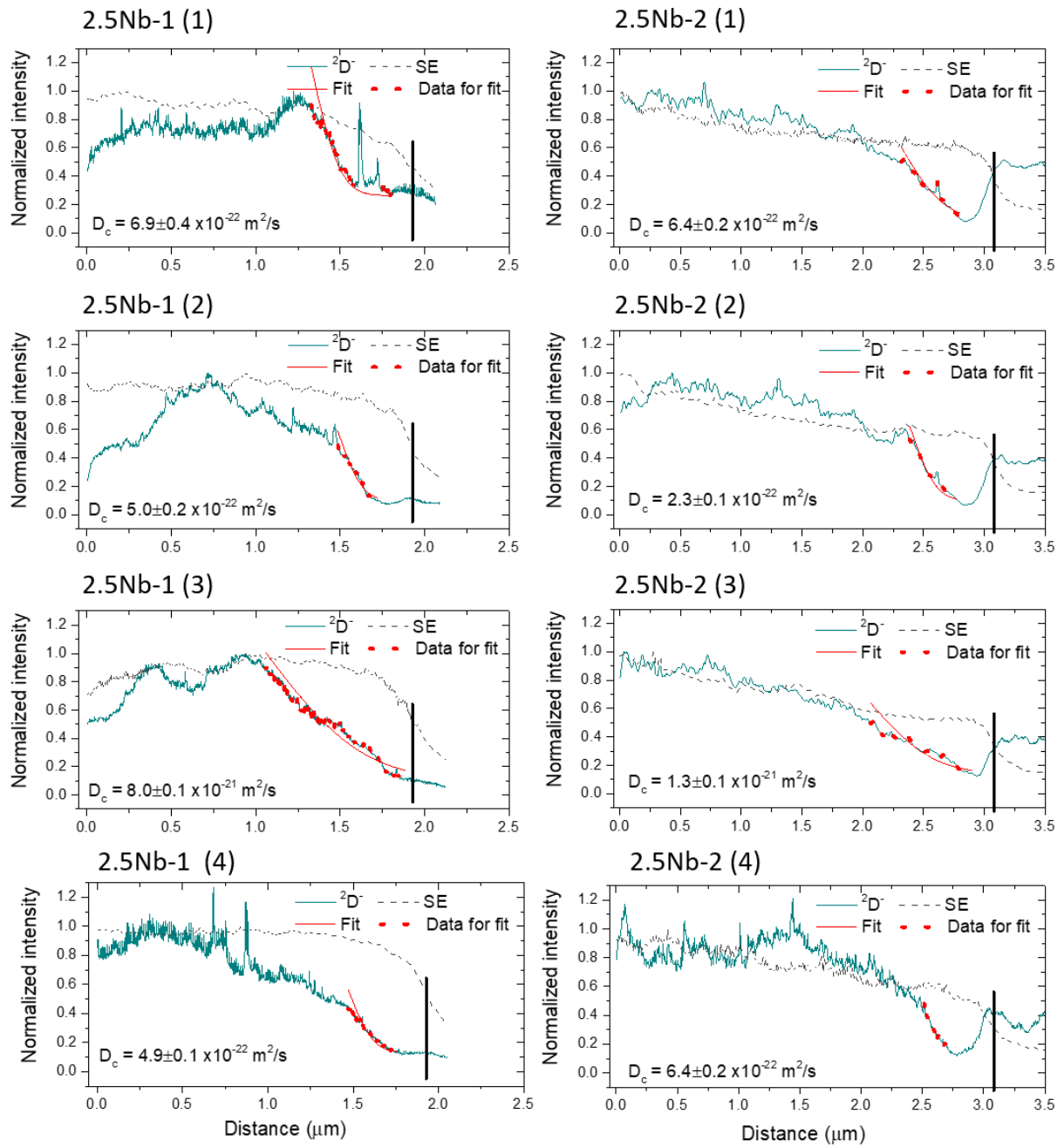Figure S5. NanoSIMS Depth profile data in samples 1Nb-1 (46-days autoclave-corroded annealed Zr-1Nb).

Figure S6. NanoSIMS Depth profile data in samples 2.5Nb-1 (left column, 150-days autoclave-corroded Zr-2.5Nb) and 2.5Nb-2 (right column, 700-days autoclave-corroded Zr-2.5Nb).
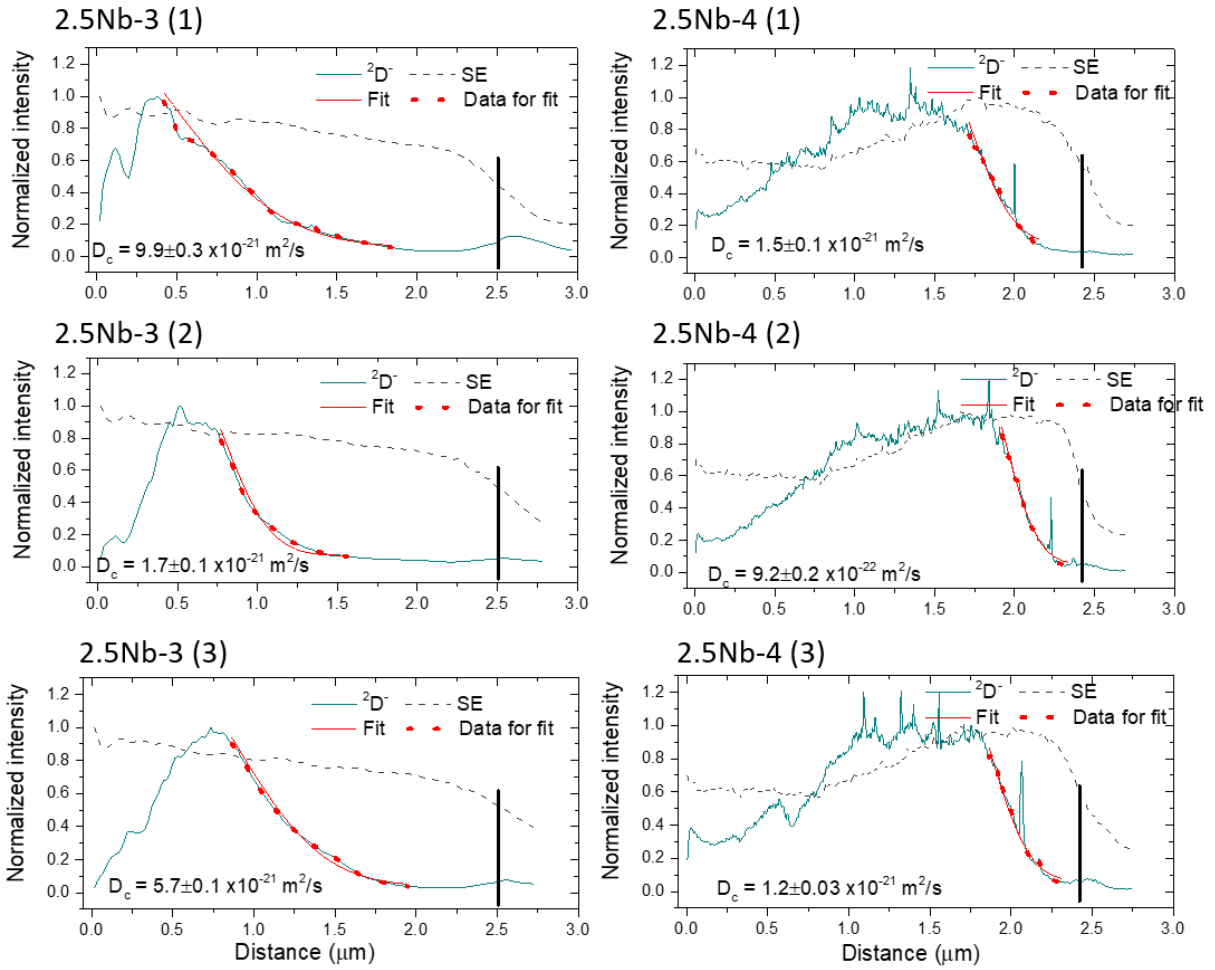
Figure S7. NanoSIMS Depth profile data in samples 2.5Nb-3 (left column, 192-days in-flux-corroded Zr-2.5Nb) and 2.5Nb-4 (right column, 185-days out-of-flux-corroded Zr-2.5Nb).
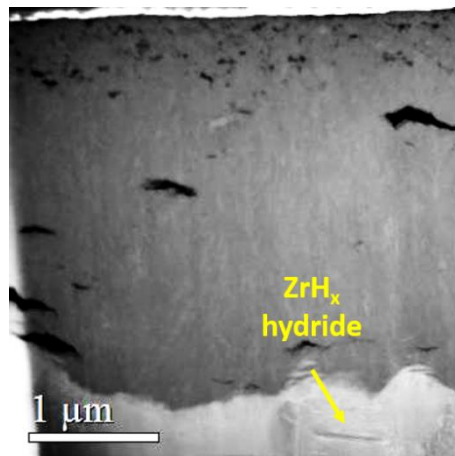

Figure S8. High-angle annular dark-field (HAADF) STEM image showing the hydrides distribution on sample Z4-2. Hydrides and oxides are darker in the HAADF mode because the Zr metal matrix has a higher average atomic mass. A hydride in the sample metal matrix of sample Z4-2 is indicated by the yellow arrow.